Journal of Applied Polymer Science

Non-isothermal crystallization kinetics of cork-polymer composites for injection molding

Sara P. Magalhães da Silva,[1,2] Paulo S. Lima,[1] José M. Oliveira[1,2]

[1]School of Design, Management and Production Technologies, University of Aveiro, Santiago de Riba-Ul, Oliveira de Azeméis 3720-509, Portugal

[2]Aveiro Institute of Materials (CICECO), University of Aveir, Campus Universitário de Santiago, 3810-193 Aveiro, Portugal

Correspondence to: S. Silva (E-mail: sarapms@ua.pt)

ABSTRACT: The non-isothermal crystallization behavior of cork–polymer composites (CPC) based on polypropylene (PP) matrix was studied. Using differential scanning calorimetry (DSC), the crystallization behavior of CPC with 15 wt % cork powder at different cooling rates (5, 10, 15, and 20 °C/min) was studied. The effect of a coupling agent based on maleic anhydride was also analyzed. A composite (PPg) containing polypropylene grafted maleic anhydride (PPgMA) and PP was prepared for comparison purposes. Crystallization kinetic behavior was studied by Avrami, Ozawa, Liu, and Kissinger methods. The Ozawa method fails to describe the behavior of these composites. Results show that cork powder surface acts as a nucleating agent during non-isothermal crystallization, while the addition of PPgMA decreases the crystallization rate. © 2016 Wiley Periodicals, Inc. J. Appl. Polym. Sci. **2016**, *133*, 44124.

KEYWORDS: compatibilization; composites; crystallization; differential scanning calorimetry (DSC); kinetics

Received 23 February 2016; accepted 20 June 2016

DOI: 10.1002/app.44124

INTRODUCTION

Given the current environmental, societal, and political situation, there is a pressing and growing need for innovative, sustainable, and recyclable materials. Cork is a technologically relevant material for the 21st century, competing in areas traditionally dominated by metal and oil derivatives. In a society that requires a more intelligent use of resources, cork is a reliable and sustainable raw material. Cork oak forests also contributes to the biodiversity of species and to the retention of CO_2.[1] Cork is the outer bark of the cork oak tree *Quercus suber L.* and its main chemical composition is based on suberin (33–50%), lignin (20–25%); polysaccharides (12–20%) and extractives (14–18%). In terms of structure, cork presents tiny hollow cells of hexagonal shape in a closed-cell foam.[2,3] It is well known that the major use for cork is the production of stoppers, which generates a relative high amount (≈30 wt %) of residues, that are usually burned.[4] These residues are suitable raw materials for the development of new materials solutions tailoring the needs of different applications. The combination of cork with polymeric matrices reveals to be a significant added-value to cork based materials. Low density, hardness and cost, good relation between strength/weight, good insulation properties, and high levels of filling are some of the advantages of applying natural materials as fillers in thermoplastic composites. They are, also, renewable and readily available materials, recyclable, and non-toxic.[4–6]

Mechanical properties of composites are highly dependent on the interaction between the polymer matrix and the filler. Coupling agents are usually applied to promote the compatibility between polymer matrices and lignocellulosic materials. PPgMA is one of the most used coupling agent in several polyolefin composites with natural fibers.[7–12] The interactions between PPgMA maleic groups and hydroxyl groups of natural fibers increase the interfacial adhesion between both materials leading to a better mechanical performance.[5,13] Composites performance depends not only on the compatibility of the matrix and filler, but also on the morphology and crystallinity. Several studies regarding morphology, mechanical, and thermal properties of PP filled with natural fibers have already been reported.[14–23] However, few studies analyzed the effect of cork on PP degree of crystallinity[5,24] and, so far, none of the studies are related to the matrix crystallization kinetics.

The final mechanical properties of composites reinforced with natural materials are partially dependent on the crystallization behavior of the matrix. Crystallization occurs through the nucleation and growth mechanisms of small molecules. The addition of natural materials can influence the crystallization process mostly by revealing nucleation activity and/or transcrystallization.[25–27] The processing conditions also affects the crystallization behavior. In industrial processes, like extrusion and injection molding, composites experience non-isothermal crystallization rather than isothermal crystallization. In injection molding, processing parameters, such as,

Table I. Cork Particles: Physical Characteristics

Granulometry mesh (μm)	Cork powder (%)	Average particle size (μm)
1000	2.3 ± 0.1	596
800	45.8 ± 0.1	
400	51.4 ± 0.1	
200	0.6 ± 0.1	

melting temperatures, pressures, and shear rates are applied during the process. These severe conditions influence the PP crystals nucleation and growth and, therefore, the spherulites number and size. The use of nucleating agents can contribute for a shorter injection molding cycle reducing the manufacturing costs. It can also improves optical and mechanical properties through the development of small spherulites.[27,28]

Soleimani *et al.*[27] studied the effect of flax fiber loading, chemical modification, and the use of compatibilizer (PPgMA) on the non-isothermal crystallization kinetics of PP. They found that the addition of flax fibers resulted in higher degree of crystallinity (X_c). This was attributed to the nucleation ability of the fibers which provides nucleation sites and facilitates crystallization of the polymer as well as transcrystallinity. Some fibers have the ability to act as heterogeneous nucleating agents promoting high density of nucleation centers. The crystals grow in a direction perpendicular to the fibers surface occurring the transcrystallinity phenomenon.[27] At the same cooling rate, the addition of fibers increased crystallization temperature (T_c). For higher cooling rates, a lower T_c and X_c were observed, but a faster kinetic of crystallization was attained. In this study,[27] PPgMA reduced the crystallinity degree, but accelerated the crystallization rate. The same trend was observed by Grozdanov *et al.*,[25] who have studied the non-isothermal crystallization kinetics of kenaf fiber/polypropylene composites.

The present study is part of a major project which aims to evaluate the feasibility of cork–polymer composites (CPC) production through a modified injection molding technology without minimizing the damage of cork structure. A rheological study of CPC with three different cork granulometries was already been analyzed.[29] This study showed that cork can be considered on the development of sustainable materials for injection molding technology. The main objective of this work is to study the crystallization kinetics of CPC under non-isothermal conditions using differential scanning calorimetry (DSC). The influence of cork presence on the nucleation and crystal growth behavior of PP was evaluated using Avrami,[30] Ozawa,[31] and Liu *et al.*[32] models. Crystallization activation energy (ΔE_c) was determined through Kissinger model.[33] CPC crystallization kinetics should be addressed to better describe the crystallization behavior during the injection molding process.

EXPERIMENTAL

Materials

Cork powder used in this work was supplied by a Portuguese cork producer. Sample was fractionated through sieving (Retsch, Germany) and the relative amount of particles according to its size was determined (Table I). No particles were retained in sieves below 100 μm. The average particle size was calculated recurring to eq. (1).

$$d_p = \frac{\sum w_i d_i^4}{\sum w_i d}{}^i i^3 \quad (1)$$

where w_i is the weight fraction in each sieve and d_i is the sieve mesh size.

The polymeric matrix used in this work is a homopolymer PP (PPH 10060) from Total Petrochemicals, with a melt flow index (MFI) of 35 g·10 min^{-1} (230 °C, 2.16 kg) and a melting point of 165 °C. The coupling agent applied was PPgMA from ExxonMobil, Germany (Exxelor™ PO 1020) containing 0.5–1.0 wt % of grafted maleic anhydride, with a MFI of 430 g 10 min^{-1} (230 °C, 2.16 kg) and a melting point of 162 °C.

Preparation of CPC

Before compounding, the cork particles were dried at 70 °C for 24 h in a vacuum oven (Carbolite AX60 model) to stabilize the moisture content. It is known that the cork structure and composition do not suffer significant changes up to 250 °C.[34] CPC were compounded in a Brabender type internal mixer. The total volume of the mixing chamber is 355 cm^3. First, PP pellets were charged and melted for 2 min at 180 °C and 40 rotations per minute. Then, cork particles were added and the materials were mixed for additional 8 min. For the preparation of CPC in the presence of coupling agent, PPgMA was added together with cork particles. A formulation of PP/PPgMA (PPg) was prepared to evaluate the individual effect of PPgMA in the PP matrix. Compositions of all samples are shown in Table II.

DSC

Crystallization behavior of all samples was carried out in a Shimadzu DSC-60 equipment. The equipment was calibrated by using indium as the reference material. Samples weights varying between 5.0 and 6.0 mg were encapsulated in aluminum pans. Each sample was heated from 20 °C to 200 °C at a scan rate of 20 °C/min and held for 2 min at this temperature to eliminate the thermal history and prevent self-seeding of PP.[35] Then, they were cooled until −80 °C and heated again up to 200 °C. Four different heating/cooling rates: 5, 10, 15, and 20 °C/min were

Table II. Compositions Used in the Preparation of CPC

Sample Code	PP (wt %)	PPgMA (wt %)	PP/PPgMA ratio	Cork (wt %)	PP/Cork ratio	(PP+PPgMA)/Cork
PPg	95	5	20	—	—	—
CPC 1	85	—	—	15	6	—
CPC 1g	83	4	20	13	6	—

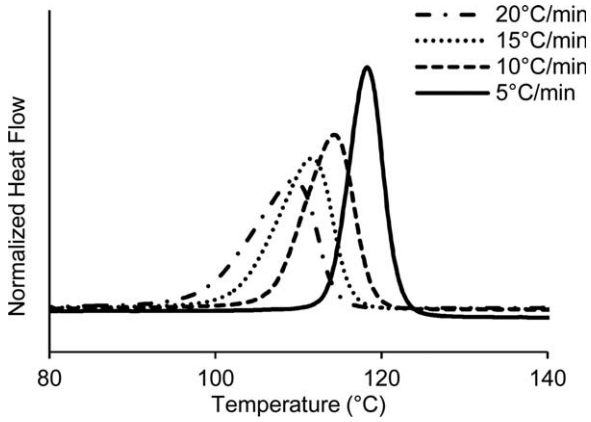

Figure 1. DSC curves of CPC 1 at different cooling rates.

used. Only the second run was considered to analyze the crystallization behavior process: crystallization temperature (T_c), endset temperature (T_e), onset temperature (T_o), and crystallization enthalpy (ΔH_c). DSC thermograms analyses were made by using TA-60WS software. The crystallinity is associated with the exothermic peaks maxima obtained by DSC.

Optical Microscopy

Observations under reflected-light microscope were carried out on a Nikon Eclipse L150. Samples were melted for 2 min in a hot plate and the crystallites morphology examined upon cooling.

RESULTS AND DISCUSSION

Non-Isothermal Crystallization Behavior

Melt crystallization exotherms of the samples at different cooling rates are presented in Figures 1 and 2. The DSC curves of CPC 1 at different cooling rates (all the other samples exhibited the same behavior—not shown) are shown in Figure 1. The DSC curves of all samples at cooling rate of 5 °C/min are displayed in Figure 2. The thermal properties of all samples are listed in Table III.

It is visible that T_c shifted to lower values as the cooling rates increase, indicating that the crystallization process occurs sooner for lower cooling rates. The crystallization peak width became narrow as the cooling rate is decreasing. This narrowing can be associated to a lower crystallites geometry dispersion, where at lower cooling rates the formation of less perfect crystallites is attained.[36]

At a given cooling rate, the values for the T_c of composites were higher than neat PP and the addition of the coupling agent resulted in an increase of T_c. At higher cooling rates, polymer chains were less movable and possessed shorter time to diffuse into the crystalline phase, which resulted in a decrease of T_c. Lower cooling rates promote conditions for better polymer crystals development due to a kinetic process. It is also known that the polymer chain length and its branches influence the crystallization process.[36]

From Figure 2 it is seen that composites materials crystallization peaks are between PP and PPg crystallization peaks, indicating that the crystallization process is governed by the polymeric matrix.

The degree of crystallinity (X_c) was calculated according to eq. (2), where the ΔH_c was obtained through the integration of the crystallization peak. ΔH_m^0 corresponds to 100% crystalline PP being equal to 207 J g^{-1} and w is the weight cork fraction in the composite.[36]

$$X_c(\%) = \frac{\Delta H_c}{\Delta H_m^0 (1-w)} \times 100 \quad (2)$$

At the same cooling rate, crystallinity increased with the addition of cork powder to PP matrix (Table III). This can be attributed to the nucleating effect of cork which provided nucleation sites and facilitated the crystallization of the polymer.[5,37] Additionally, at the same cooling rate the presence of cork also increased T_c.

The use of PPgMA, not only attributes for the increasing of the degree of crystallinity of PPg and CPC 1g, but also the time needed to achieve 50% extent of crystallization (defined as half-time crystallization ($t_{1/2}$), which is obtained directly from the plot of relative degree of crystallinity (X_t vs. time). These results show that, although, the addition of PPgMA leads to higher crystallinities, it is observed that non-isothermal crystallization occurred faster in neat PP and CPC 1. This means that, however, more crystals are growing, they're growing very slowly, which reduces the overall crystallization rate.

Zhang *et al.*[38] proposed the crystallization rate parameter (CRP), which can be used to quantitatively compare the non-isothermal crystallization rate. CRP can be determined by the slope of a linear plot of $1/t_{1/2}$ versus cooling rate. A higher slope implies a faster crystallization rate.

Figure 3 shows the plots of $1/t_{1/2}$ vs. cooling rate and CRP values are displayed in Table III. CPC 1 presented the higher CRP value, proving the nucleating effect of cork. The presence of the coupling agent reduced the crystallization rate, probably due to the increased interactions between cork-PP in the presence of PPgMA. As the degree of grafting increases, the mobility of polymer chains segments decreases hindering the crystallization rate.[25]

The relative degree of crystallinity (X_t), as a function of temperature, is determined applying eq. (3), where T_0 and T_∞ are the onset and end temperatures, respectively.

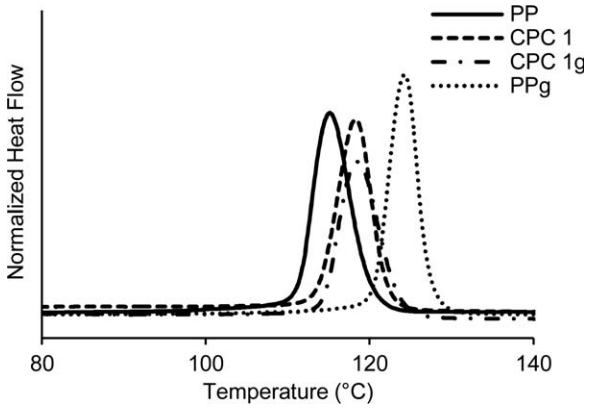

Figure 2. DSC curves of all samples at 5 °C/min.

Table III. Non-Isothermal Crystallization Parameters Obtained by DSC (R2—Correlation Coefficient)

Sample	φ (°C min^{-1})	T_0 (°C)	T_c (°C)	X_c (%)	$t_{1/2}$ (s)	CRP	R^2
PP	5	122.8	114.8	49.7	100	0.086	0.987
	10	114.0	106.1	41.5	54		
	15	111.5	103.6	40.1	38		
	20	109.2	99.2	39.0	32		
PPg	5	133.4	124.7	52.4	125	0.084	0.980
	10	127.6	120.0	50.7	61		
	15	125.5	118.2	48.2	41		
	20	124.6	116.9	47.5	35		
CPC 1	5	124.1	118.5	50.0	82	0.095	0.995
	10	121.5	114.6	49.8	48		
	15	120.0	111.6	50.7	34		
	20	118.5	108.8	50.6	28		
CPC 1g	5	126.1	119.0	53.0	97	0.060	0.994
	10	123.5	114.8	53.8	62		
	15	120.5	111.9	50.7	44		
	20	119.9	109.8	52.0	37		

$$X_t = \frac{\int_{T_0}^{T} \left(\frac{dH_c}{dT}\right) dT}{\int_{T_0}^{T_\infty} \left(\frac{dH_c}{dT}\right) dT} \quad (3)$$

During the non-isothermal crystallization process, the relation between crystallization time (t) and temperature is given by eq. (4), in which φ is the cooling rate.

$$t = \frac{|T_0 - T|}{\varphi} \quad (4)$$

Curves of relative crystallinity as function of time for all the studied samples are presented in Figure 4. At different cooling rates all curves have the same sigmoidal shape.

The first nonlinear part is usually considered the nucleation step of the crystallization process.[39] The longest nucleation step occurs for PPg sample (5 °C/min), which indicates that more nuclei were formed. PPgMA presence seems to induce the formation of more nuclei for crystal growth. In this case, a fast primary crystallization occurred in the early stage, while a slower secondary crystallization at the latter stage is observed. The curvature of this second nonlinear part leveled off, which was probably caused by the spherulite impingement or crowding in the late stage of crystal growth.[40,41] Higher cooling rates managed to complete the crystallization process in a shorter time. This behavior is also observed through the $t_{1/2}$ parameter (Table III). It is visible that, $t_{1/2}$ decreased with the increase of cooling rate, indicating that a shorter time is needed to achieve 50% extent of crystallization.

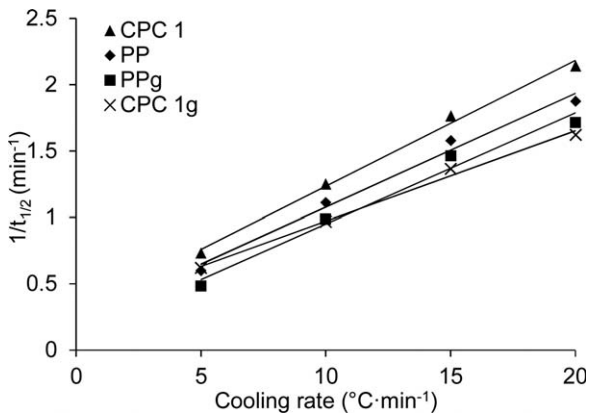

Figure 3. Plots of 1/t1/2 vs. cooling rate of all samples.

Non-Isothermal Crystallization Kinetics

The Avrami[30] model is commonly used to describe the isothermal crystallization kinetic behavior:

$$1 - X_t = \exp(-Z_t t^n) \quad (5)$$

where Z_t is the crystallization rate constant containing the nucleation and growth rates and it is temperature dependent; n is the Avrami index which depends on the type of nucleation and growth process. The linearized form can be written as:

$$\log[-\ln(1 - X_t)] = \log(Z_t) - n \log(t) \quad (6)$$

Mandelkern[42] considered that the primary non-isothermal crystallization stage can be described through this model, based on a constant crystallization temperature assumption. The n and Z_t parameters do not have the same physical meaning as in the isothermal crystallization processes, since the temperature changes steadily during a non-isothermal crystallization. Nucleation and crystal growth are temperature dependent, and a temperature change at a given cooling rate affects the kinetics of both processes. Jeziorny[43] calibrated the Z_t parameter, considering the temperature dependence of the non-isothermal crystallization:

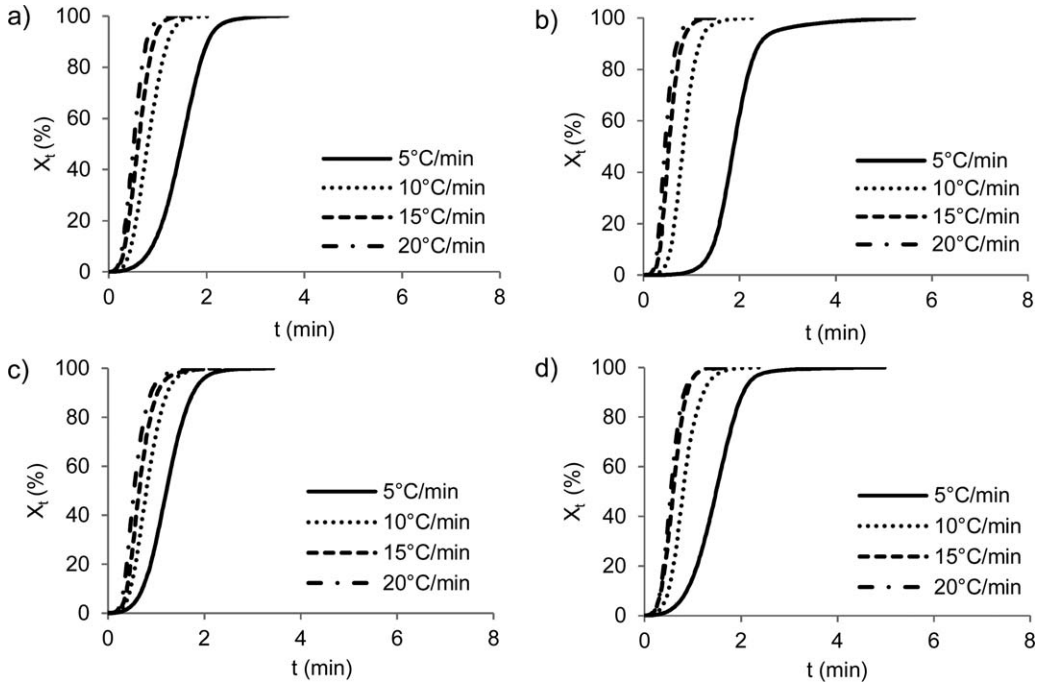

Figure 4. Relative crystallinity (X_t) vs. time (t) curves of the samples: (a) PP, (b) PPg, (c) CPC 1, and (d) CPC 1g.

$$\log Z_c = \frac{\log(Z_t)}{\varphi} \tag{7}$$

Avrami plots are shown in Figure 5 and the kinetic parameters are presented in Table IV. In the fitting, it was considered X_t values between 10 and 90%.

The variation of the Avrami parameter n with cooling rate indicates the presence of a growth and nucleation mixed mechanism. According to literature, n should be an integer value varying from 1 to 4.[44] A non-integer value also designates a crystallization process in various growth forms, indicating that the nucleation/crystallization mechanisms are difficult to be established in a single way and, additional information must be obtained. The determination of n depends upon factors, such as, volume changes due to phase transformation, incomplete crystallization, annealing, or different mechanisms involved during the process.[45] In this study, the n values variation indicate a three-dimensional growth mechanism.[46] However, non-integer values were obtained and a more detailed analysis is required to evaluate the specific nucleation mechanism.

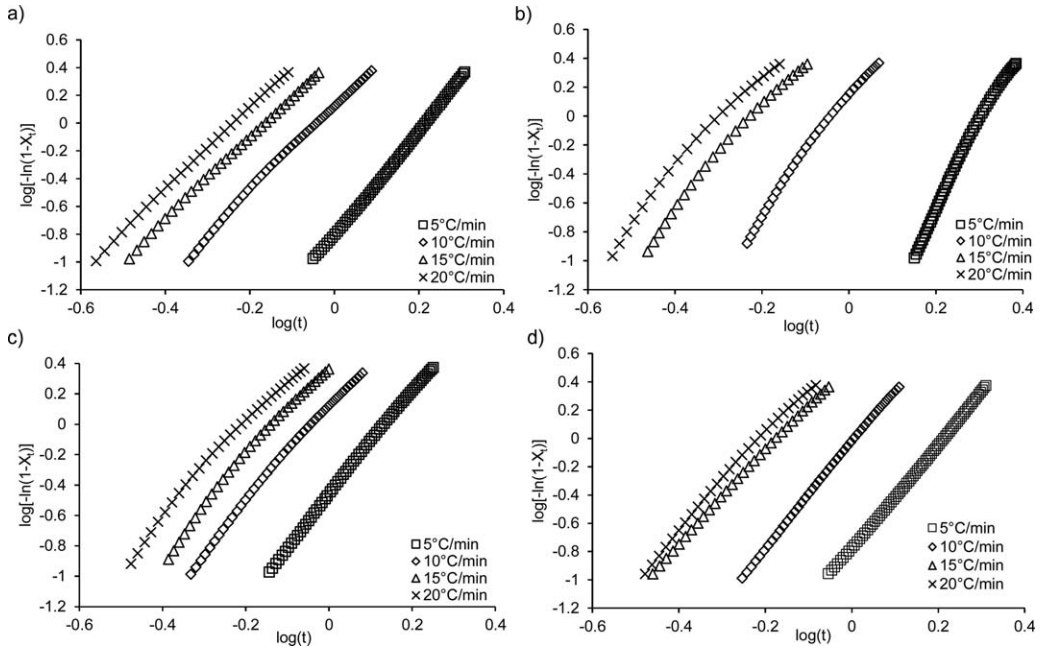

Figure 5. Avrami plots of the samples: (a) PP, (b) PPg, (c) CPC 1, and (d) CPC 1g.

Table IV. Avrami Kinetic Parameters

Samples	φ (°C min^{-1})	N	Z_c (min °C^{-1})	R^2
PP	5	3.79	0.689	0.994
	10	3.09	1.034	0.997
	15	2.93	1.113	0.999
	20	2.96	1.117	0.999
PPg	5	5.89	0.434	0.993
	10	4.08	1.030	0.992
	15	3.45	1.077	0.993
	20	3.32	1.085	0.993
CPC 1	5	3.45	0.808	0.999
	10	3.18	1.029	0.996
	15	3.14	1.085	0.993
	20	2.90	1.091	0.992
CPC 1g	5	3.67	0.699	1.000
	10	3.75	0.994	1.000
	15	3.26	1.065	0.999
	20	3.39	1.070	0.996

The rate parameter Z_c increases with increasing cooling rate, meaning an increase in crystallization rate. When compared to neat PP, an increase of Z_c values is observed for CPC 1, suggesting an increase in the heterogeneous crystallite nucleation rate.[40] Contrarily, the addition of PPgMA revealed a decrease in Z_c.

Ozawa[31] extended the Avrami model to describe the non-isothermal processes [eq. (8)] by assuming infinitesimally small changes in the isothermal crystallization steps and obtained:

$$1-X_t=\exp\left(-\frac{K(T)}{\varphi^m}\right) \tag{8}$$

where m is the Ozawa exponent, which is dependent on the nucleation density. The spherulitic radial growth rate and $K(T)$ is a function of the overall crystallization rate. The linearized form of the model is shown in eq. (9).

$$\ln[-\ln(1-X_t)]=\ln K(T)-m\ln(\varphi) \tag{9}$$

The Ozawa model is one of the most used models for studying non-isothermal crystallization kinetics. Ozawa plots for CPC 1 at different crystallization temperatures are represented in Figure 6. It is clearly seen that in the presence of cork, the Ozawa plots are nonlinear and so, the Ozawa model could not be used to describe adequately the non-isothermal crystallization of PP/cork composites. The reason why this happened was attributed to the secondary crystallization stage that occurs during non-isothermal crystallization process of PP in the presence of cork. In a study by Grozdanov *et al.*,[25] where they studied the non-isothermal crystallization kinetics of kenaf fiber/polypropylene composites, they found the same behavior when fitted the data to the Ozawa model. They explain this non-linearity by the fact that for different cooling rates and at a given temperature, the crystallization processes are at different stages. More specifically, at lower cooling rates, the process is at the end of the crystallization, while at higher cooling rates, the crystallization is at an early stage. Xu and coworkers[26] when analysed the non-isothermal crystallization kinetics of PP composites reinforced with down feather fibers had the same Ozawa non-linearity tendency. The fact that Ozawa's model does not consider the slow secondary crystallization was considered as the reason for this behavior.

The description of the non-isothermal crystallization kinetics only by a single method is non-effective, once several parameters need to be taken into account simultaneously. Liu *et al.*[32] proposed an alternative method through the combination of Avrami and Ozawa models [eq. (10)] based on the fact the relative degree of crystallinity is correlated to the cooling rate and crystallization time.

$$\log(\varphi)=\log[F(T)]-\alpha\log(t) \tag{10}$$

where $F(T)=[K(T)/Z_t]^{1/m}$ [eq. (11)] refers to the cooling rate value in which the system reaches a certain degree of crystallinity in the unit of time, while α is the ratio between Avrami and Ozawa exponents ($\alpha = n/m$).

Liu's approach plots are given in Figure 7 and the corresponding parameters are presented in Table V. A small variation of α and a R^2 closer to one reveals that Liu's method was capable to describe accurately the non-isothermal crystallization of the analyzed materials. Values of α closer to 1 were obtained for PP, PPg, and CPC 1g samples, indicating that Avrami and Ozawa exponents are similar. It also discloses that the ratio of crystallization between 5 °C/min and 20 °C/min is constant whatever the relative crystallinity (see Figure 7).

For CPC 1, α values were closer to 2, which means that Avrami exponent is superior than Ozawa exponent. As referred above, a n value between 2 and 3 can indicate a three-dimensional crystallization growth. Furthermore, the crystallization ratio increased reinforcing the idea of cork as a nucleating agent.

$F(T)$ value increased as the relative crystallinity increases, since the motion of molecular chains became slower as the material crystallized and the formation of new crystals is hampered.[40] Higher $F(T)$ values imply a slower crystallization rate. CPC 1 presented the lowest $F(T)$ values, indicating a faster crystallization rate when cork is added to the PP matrix. This result confirms, once again, the nucleating ability of cork. On the other

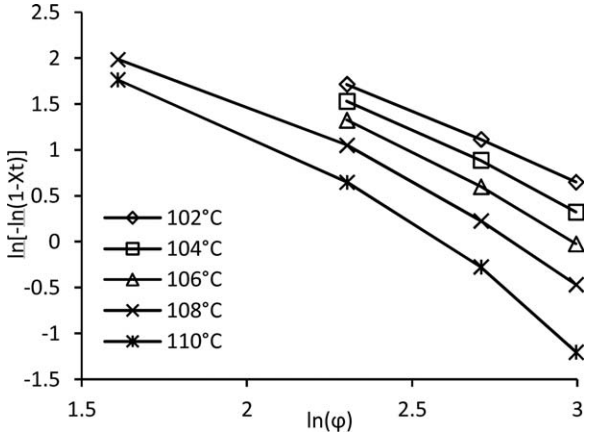

Figure 6. Ozawa plot for CPC 1 at different crystallization temperatures.

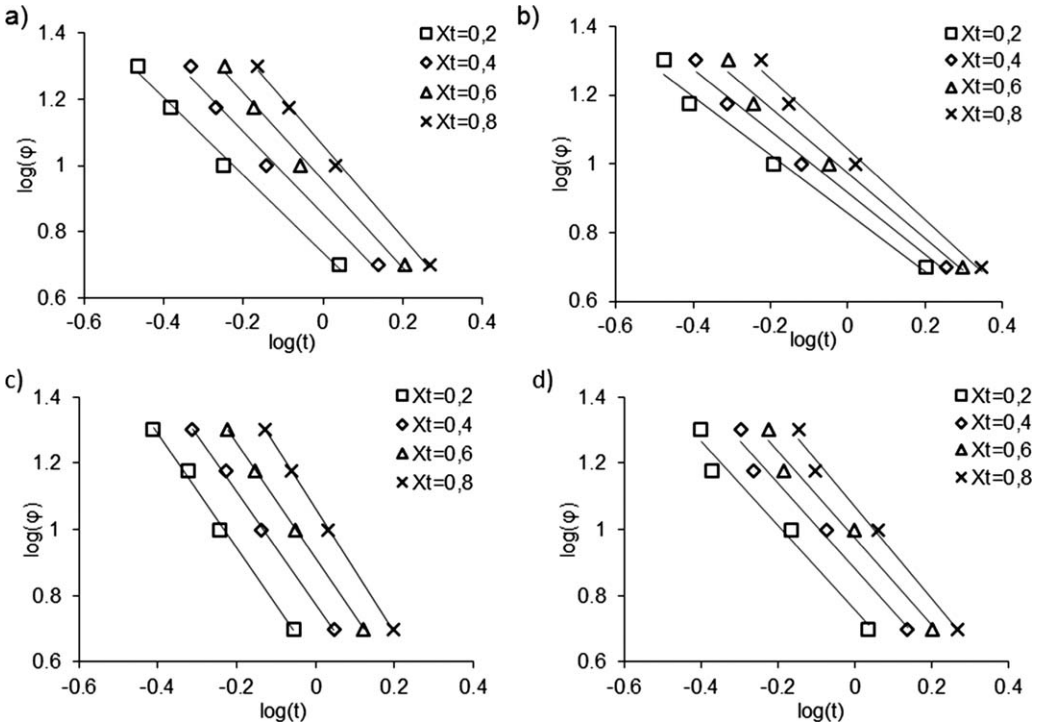

Figure 7. Liu plots of the samples: (a) PP, (b) PPg, (c) CPC 1, and (d) CPC 1g.

hand, the addition of PPgMA decreased the crystallization rate (both for PPg and CPC 1g). As discussed before, the increased interactions between cork and PP due to the presence of PPgMA resulted in a decreased mobility of the polymer chains and, consequently, the crystallization rate is hindered. The results obtained from this model are in agreement with those obtained by the Avrami model.

According to Vyazovkin and Sbirrazzuoli,[47] the Kissinger model[33] [eq. (11)] seems not to be the most efficient method to evaluate crystallization activation energy (ΔE_C). Although in order to compare the activation energy with similar studies, the Kissinger method was used. ΔE_C is the activation energy required for transportation of molecular segments from melt to the crystal growth surface.

Table V. Liu's Kinetic Parameters

Sample	X_t	α	$F(T)$	R^2
PP	0.2	1.17	5.43	0.99
	0.4	1.24	7.18	0.99
	0.6	1.32	9.00	0.99
	0.8	1.39	11.50	1.00
PPg	0.2	0.85	7.21	0.99
	0.4	0.90	8.24	0.99
	0.6	0.95	9.37	0.99
	0.8	1.02	10.99	0.99
CPC 1	0.2	1.72	3.98	1.00
	0.4	1.70	5.97	1.00
	0.6	1.74	8.13	1.00
	0.8	1.86	11.53	1.00
CPC 1g	0.2	1.27	5.73	0.98
	0.4	1.29	7.63	0.98
	0.6	1.32	9.43	0.98
	0.8	1.39	11.78	0.99

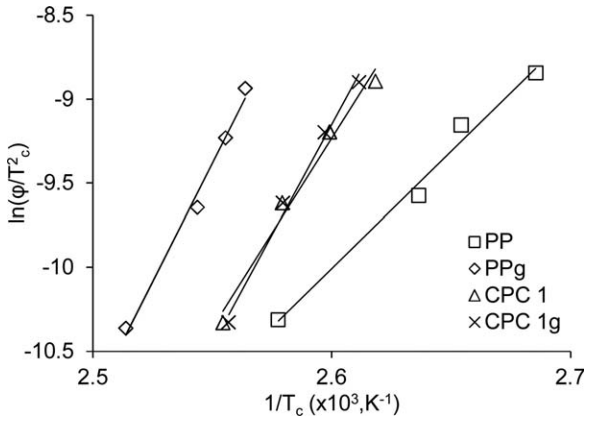

Figure 8. Kissinger plots of the samples.

Table VI. Crystallization Activation Energy (ΔE_C) of Samples

Sample	ΔE_C (kJ mol^{-1})	R^2
PP	−115.71	0.99
PPg	−233.84	0.99
CPC 1	−187.47	0.98
CPC 1g	−217.88	0.99

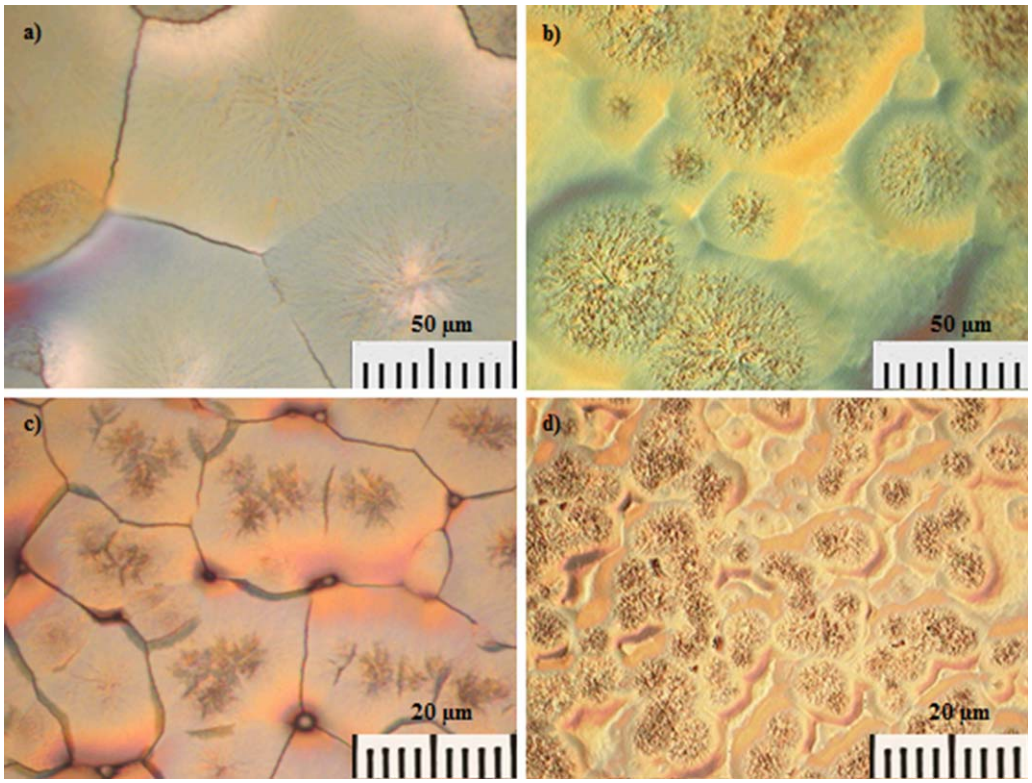

Figure 9. Optical micrographs of the samples: (a,c) pure PP and (b,d) PP in the presence of cork. [Color figure can be viewed in the online issue, which is available at wileyonlinelibrary.com.]

$$\frac{-\Delta E_C}{R} = \frac{d\left(\ln\left(\frac{\varphi}{T_c^2}\right)\right)}{d\left(\frac{1}{T_c}\right)} \tag{11}$$

where R is the gas constant and T_c is the crystallization temperature.

Kissinger plots are visible in Figure 8 and the corresponding ΔE_C values are listed in Table VI. The ΔE_C values are negative owing to the exothermic character of the transition from melt to crystalline state. From these negative values, we can also infer an increase of crystallization with decreasing temperatures, revealing a barrierless crystallization process.[41] The addition of cork resulted in a decrease of the ΔE_C compared to neat PP, indicating a faster crystallization rate in the presence of cork. Soleimani *et al.*[27] reported that biofibers act as high energy sites lowering the activation energy needed for nucleation. The low ΔE_C values for composites are in agreement with theirs higher crystallinity degree (see Table III).

Optical Microscopy Analysis

Optical microscopy analysis was performed to visualize the nucleating ability of cork. Optical micrographs of pure PP and PP in the presence of cork powder at different magnifications are shown in Figure 9. The results suggest differences between the number and dimension of crystallites when PP crystallizes in the presence of cork. A higher number of crystallites with smaller dimensions is seen when PP crystallizes in the presence of cork, supporting the nucleating ability of cork already checked through the non-isothermal crystallization analyses. In semi-crystalline polymer composites reinforced with natural fibers it is usually observed a typical nucleation morphology: transcrystallinity.[48] However, in this case no transcrystalline layer on cork was found. The same observation was reported by Fernandes *et al.*[24]

CONCLUSIONS

The non-isothermal crystallization behaviors of PP, PPg, and CPC were investigated at different cooling rates (5, 10, 15, and 20 °C/min) through DSC measurements. It was found that the crystallization behavior was affected by the different cooling rates. At higher cooling rates, the crystallization occurred at lower temperatures. Avrami, Ozawa, Liu, and Kissinger methods were applied to analyze the non-isothermal kinetics of all samples. Avrami and Liu methods successfully described the non-isothermal crystallization processes of PP and composites, while the Ozawa model failed, due to the secondary crystallization stage. The addition of cork increased the crystallization rate of PP matrix and the Avrami parameter n was between 2 and 3, indicating a three-dimensional crystallization growth (also supported by optical microscopy). On the other hand, in the presence of PPgMA, the crystallization rate is hindered, owing to the introduction of maleic anhydride group. Even though the crystallinity degrees at all cooling rates for composites with PPgMA are higher, theirs $t_{1/2}$ increased, meaning that, although more crystals are growing, they're growing more slowly, which reduces the overall crystallization rate.

The present study allowed to understand the effect of different cooling rates on CPC non-isothermal crystallization process.

ACKNOWLEDGMENTS

The authors are grateful to COMPETE—Programa Operacional Factores de Competitividade (POFC), project number 30176, for financial support.

REFERENCES

1. Gil, L. *Front. Chem.* **2014**, *2*, 16.
2. Pereira, H. Cork: Biology, Production and Uses; Elsevier: Amsterdam, **2007**; p 33.
3. Silva, S. P.; Sabino, M. A.; Fernandes, E. M.; Correlo, V. M.; Boesel, L. F.; Reis, R. L. *Int. Mater. Rev.* **2005**, *50*, 345.
4. Fernandes, E. M.; Aroso, I. M.; Mano, J. F.; Covas, J. A.; Reis, R. L. *Compos. Part B: Eng.* **2014**, *67*, 371.
5. Fernandes, E. M.; Correlo, V. M.; Mano, J. F.; Reis, R. L. *Compos. Part B: Eng.* **2014**, *66*, 210.
6. Pracella, M.; Haque, M. U.; Alvarez, V. *Polymers (Basel)* **2010**, *2*, 554.
7. Gassan, J.; Bledzki, A. K. *Compos. Part A: Appl. Sci. Manuf.* **1997**, *28*, 1001.
8. Feng, D.; Caulfield, D. F.; Sanadi, A. R. *Polym. Compos.* **2001**, *22*, 506.
9. Espert, A.; Camacho, W.; Karlson, S. *J. Appl. Polym. Sci.* **2003**, *89*, 2353.
10. Soccalingame, L.; Bourmaud, A.; Perrin, D.; Bénézet, J. C.; Bergeret, A. *Polym. Degrad. Stabil.* **2015**, *113*, 72.
11. Mishra, S.; Verma, J. *J. Appl. Polym. Sci.* **2006**, *101*, 2530.
12. Pal, K.; Mukherjee, M.; Frackowiak, S.; Kozlowski, M.; Das, C. K. *J. Vinyl Addit. Technol.* **2014**, *20*, 24.
13. Tazi, M.; Erchiqui, F.; Godard, F.; Kaddami, H.; Ajji, A. *J. Appl. Polym. Sci.* **2014**, *131*. DOI: 10.1002/app.40495.
14. Nekhlaoui, S.; Essabir, H.; Kunal, D.; Sonakshi, M.; Bensalah, M. O.; Bouhfid, R.; Qaiss, A. *Polym. Compos.* **2015**, *36*, 675.
15. Tanjung, F. A.; Husseinsyah, S.; Hussin, K. *Fibers Polym.* **2014**, *15*, 800.
16. Gupta, A. K.; Biswal, M.; Mohanty, S.; Nayak, S. K. *Fibers Polym.* **2014**, *15*, 994.
17. Chaharmahali, M.; Hamzeh, Y.; Ebrahimi, G.; Ashori, A.; Ghasemi, I. *Polym. Bull.* **2013**, *71*, 337.
18. Luo, S.; Cao, J.; Peng, Y. *Polym. Compos.* **2014**, *35*, 201.
19. Wang, C.; Ying, S. *Fibers Polym.* **2014**, *15*, 117.
20. Jeencham, R.; Suppakarn, N.; Jarukumjorn, K. *Compos. Part B: Eng.* **2014**, *56*, 249.
21. Thakur, V. K.; Nayak, S. K.; Dixit, G. In Lignocellulosic Polymer Composites: Processing, Characterization and Properties; Thakur, V. K., Ed.; Wiley: New Jersey; **2014**; p 523.
22. Amieva, E. J. C.; Velasco-Santos, C.; Martinez-Hernandez, A.; Rivera-Armenta, J.; Mendoza-Martinez, A.; Castano, V. *J. Compos. Mater.* **2014**, *49*, 275.
23. Pang, M. M.; Pun, M. Y.; Ishak, Z. A. M. *Polym. Eng. Sci.* **2014**, *54*, 1357.
24. Fernandes, E. M.; Correlo, V. M.; Chagas, J. A. M.; Mano, J. F.; Reis, R. L. *Compos. Sci. Technol.* **2010**, *70*, 2310.
25. Grozdanov, A.; Buzarovska, A.; Bogoeva-Gaceva, G.; Avella, M.; Errico, M. E.; Gentile, G. *Polym. Eng. Sci.* **2007**, *47*, 745.
26. Liu, X.; Tang, Y.; Zhang, B.; Chen, F.; Xu, W. *Polym. Compos.* **2015**, 1. DOI: 10.1002/pc.23508.
27. Soleimani, M.; Tabil, L.; Panigrahi, S.; Oguocha, I. In Thermoplastic—Composite Materials; El-Sonbati, A. P., Ed.; InTech: Croatia, **2012**; p 131.
28. Mucha, M.; Królikowski, Z. *J. Therm. Anal. Calorim.* **2003**, *74*, 549.
29. Magalhães da Silva, S. P.; Lima, P. S.; Oliveira, J. M. *Compos. Part B: Eng.* **2016**, *90*, 172.
30. Avrami, M. *J. Chem. Phys.* **1939**, *7*, 1103.
31. Ozawa, T. *Polymer (Guildf)* **1971**, *12*, 150.
32. Liu, T.; Mo, Z.; Wang, S.; Zhang, H. *Polym. Eng. Sci.* **1997**, *37*, 568.
33. Kissinger, H. E. *J. Res. Natl. Bur. Stand.* **1956**, *57*, 217.
34. Rosa, M. E.; Fortes, M. A. *J. Mater. Sci. Lett.* **1988**, *7*, 1064.
35. Zheng, G.; Jia, Z.; Li, S.; Dai, K.; Liu, B.; Zhang, X.; Mi, L.; Liu, C.; Chen, J.; Shen, C.; Peng, X.; Li, Q. *Polym. Int.* **2011**, *60*, 1434.
36. Ehrenstein, G. W.; Riedel, G.; Trawiel, P. Thermal Analysis of Plastics: Theory and Practise; Hanser Gardner Publications: Nuremberg, **2004**; p 12.
37. Fernandes, E. M.; Correlo, V. M.; Mano, J. F.; Reis, R. L. *Mater. Des.* **2015**, *82*, 282.
38. Zhang, R.; Zheng, H.; Lou, X.; Ma, D. *J. Appl. Polym. Sci.* **1994**, *51*, 51.
39. Ding, W.; Chu, R. K. M.; Mark, L. H.; Park, C. B.; Sain, M. *Eur. Polym. J.* **2015**, *71*, 231.
40. Abdel Aziz, M. S.; Saad, G. R.; Naguib, H. F. *Thermochim. Acta* **2015**, *605*, 52.
41. Şanlı, S.; Durmus, A.; Ercan, N. *J. Appl. Polym. Sci.* **2012**, *125*, E268.
42. Mandelkern, L. Methods of Experimental Physics; Academic Press: New York, **1980**; p 81.
43. Jeziorny, A. *Polymer (Guildf)* **1978**, *19*, 1142.
44. Alamo, R. G.; Mandelkern, L. *Macromolecules* **1991**, *24*, 6480.
45. Di Lorenzo, M. L.; Silvestre, C. *Prog. Polym. Sci.* **1999**, *24*, 917.
46. Huang, Y.; Liu, H.; He, P.; Yuan, L.; Xiong, H. *J. Appl. Polym. Sci.* **2010**, *116*, 2119.
47. Vyazovkin, S.; Sbirrazzuoli, N. *Macromol. Rapid Commun.* **2004**, *25*, 733.
48. Quan, H.; Li, Z. M.; Yang, M. B.; Huang, R. *Compos. Sci. Technol.* **2005**, *65*, 999.